Vibrational Analysis of Amino Acids and Short Peptides in Hydrated Media. 3. Successive KL Repeats Induce Highly Stable β-Strands Capable of Forming Non-H-Bonded Aggregates

ARTICLE *in* THE JOURNAL OF PHYSICAL CHEMISTRY B · FEBRUARY 2008

Impact Factor: 3.3 · DOI: 10.1021/jp0767967 · Source: PubMed

6 AUTHORS, INCLUDING:

Belén Hernández
Université Paris 13 Nord
39 PUBLICATIONS **375** CITATIONS
SEE PROFILE

Giulia C. Fadda
Université Paris 13 Nord
17 PUBLICATIONS **146** CITATIONS
SEE PROFILE

Mahmoud Ghomi
Université Paris 13 Nord
112 PUBLICATIONS **1,774** CITATIONS
SEE PROFILE

Vibrational Analysis of Amino Acids and Short Peptides in Hydrated Media. 3. Successive KL Repeats Induce Highly Stable β-Strands Capable of Forming Non-H-Bonded Aggregates

Guy Guiffo-Soh,[†,‡] Belén Hernández,[†,‡] Yves-Marie Coïc,[§] Fatima-Zohra Boukhalfa-Heniche,[†,‡,||] Giulia Fadda,[†,‡] and Mahmoud Ghomi*[,†,‡]

UMR CNRS 7033, BioMoCeTi, UFR SMBH, Université Paris 13, 74 rue Marcel Cachin, 93017 Bobigny cedex, France, Université Pierre et Marie Curie, Case 138, 4 Place Jussieu, 75252 Paris cedex 05, France, and Unité de Chimie Organique, Institut Pasteur, 28 rue du Docteur Roux, 75724 Paris cedex 15, France

Received: August 24, 2007; In Final Form: October 29, 2007

Circular dichroism (CD) and Raman scattering were applied to the aqueous solution of minimalist LK peptides constructed with successive KL repeats leading to the following generic primary sequence: $(KL)_nK$. Three peptides of this family, a 3-mer ($n = 1$), a 9-mer ($n = 4$), and a 15-mer ($n = 7$), are analyzed in this report. Raman spectra of the 3-mer (KLK, a random chain) and its labile-hydrogen deuterated species yield a set of interesting information for analyzing longer peptides of this series. Although the CD spectrum of the 9-mer (KLKLKLKLK) reveals a signal traditionally assigned to a random structure, the corresponding Raman spectrum allows finding a mixture of conformations in solution, adopting predominantly β-type structures. This fact proves the utility of Raman spectroscopy to eliminate eventual ambiguity concerning conformational assignments in peptides based only on the use of CD technique. Finally, the 15-mer (KLKLKLKLKLKLKLK) gives rise to CD and Raman spectra clearly assignable to a β-type structure. On the basis of all the observed results on the 15-mer, we can confirm that this peptide may exist as isolated β-strands at low concentration (sub-micromolar), flat-oriented at the air/water interface, whereas at high concentrations (millimolar), non-H-bonded immersible aggregates might be formed. A hypothetical model for these β-strand aggregates could be proposed as stabilized by an interior hydrophobic core and a hydrophilic external face, formed by leucine and lysine side chains, respectively.

I. Introduction

Conformational adaptability of a peptide is monitored by physicochemical properties of its building residues and its environment. In this paper and an accompanying one[1] (part 2 of this series) we have undertaken a secondary structure investigation of *minimalist cationic peptides* formed by only two types of amino acids: leucine (L, hydrophobic residue) and lysine (K, hydrophilic residue). Both of the constituting amino acids possess large size side chains capable of taking part in intra- and interstrand interactions. In our recent report,[1] we showed the capability of the LK peptides formed by successive KLLL repeats to induce helical conformation in the peptide chains containing at least 15 amino acids. The capability of LK peptides, especially those forming α-helices in solution, to interact with membranes is now evidenced through various studies at molecular and cellular levels.[2−11] Antimicrobial property of these peptides[2,3,6−10,12] as well as their capacity in nucleic acid delivery[5,11] were evidenced. We have also reported for the first time the ability of a 15-mer peptide with KLLL repeat, i.e., $KLL(KLLL)_2KLLK$, to translocate with low toxicity a nonspecific phosphorothioate oligodeoxynucleotide into glioma cells.[11]

In the present report attention is paid to another series of minimalist LK peptides, i.e., those with the primary sequence $(KL)_nK$. The biological activity of this family of peptides has been evidenced through the analysis of their hemolytic and antibacterial effects as a function of their chain lengths ($n = 4-7$).[10] This activity was however shown to be lower than that corresponding to the helix forming LK peptides with the primary sequence $KLL(KLLL)_nKLLK$.[10] From the structural point of view, this work was motivated by the previous results on the structural behavior as well as peptide/lipid interactions of four peptides of this family using physicochemical techniques such as Langmuir film balance, FT-IR, polarization modulation IR spectroscopy (PMIRRAS),[8] and molecular modeling.[13] It was concluded that the peptides corresponding to $n = 4-7$ (9-mer to 15-mer) do the following: (i) show an ordered chain whose β-type character is reinforced with their chain length and (ii) adopt antiparallel β-sheet secondary structure, flat-oriented with respect to the air/water and the air/lipid interfaces. Some questions can be raised on the relationship and correlation between the results obtained in the above-mentioned report: (i) FT-IR experiments were performed on the solid bulk samples obtained after evaporation of methanolic solutions, (ii) PMIRRAS experiments were carried out on much less concentrated samples (sub-micromolar range). We have recently shown that the chain length, concentration, molecular environment, and time can all play an important role in the secondary structure of LK peptides.[14] All these considerations led us to overview in the present work the structural features of a representative number of $(KL)_nK$ peptides in aqueous solution and preferentially at the same concentration. In our last reports devoted to short peptides,[1,11,14] the adequacy of joint use of CD and Raman spectroscopies to analyze the peptide secondary structure with less ambiguity has been described by the combination of the

* To whom correspondence should be addressed. E-mail: ghomi@smbh.univ-paris13.fr. Tel.: +33-1-48388928. Fax: +33-1-48387356.
† Université Paris 13.
‡ Université Pierre et Marie Curie.
§ Institut Pasteur.
|| Present address: EA 3817, LNPC, UFR Biomédicale, Université Paris Descartes, 45 rue des Saints Pères, 75270 Paris cedex 06, France.

10.1021/jp0767967 CCC: $40.75
Published on Web 01/05/2008

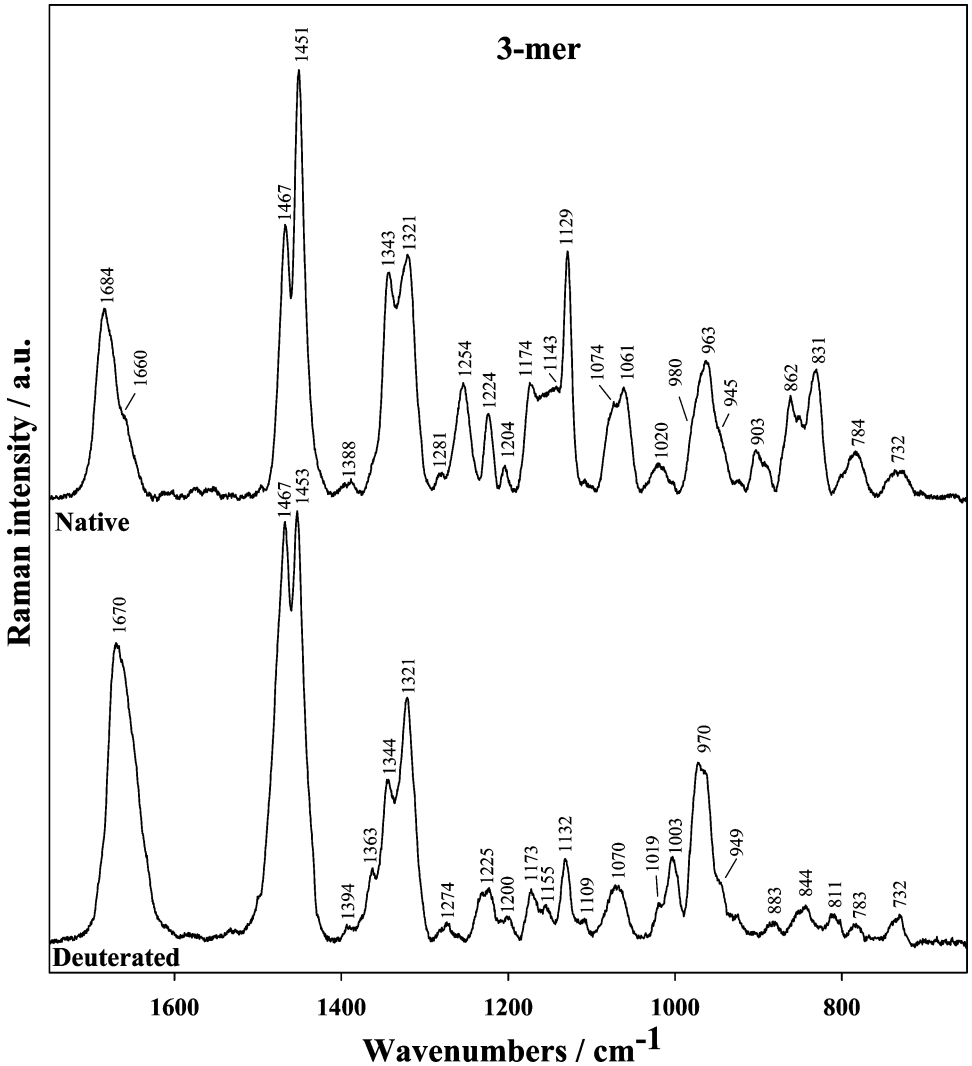

Figure 1. Room-temperature Raman spectra of the 3-mer KLK (5 mM) recorded in phosphate buffer. Spectra from native (top) and labile hydrogen deuterated (bottom) species are reported as each one being normalized to the most intense band.

data there presented. Moreover, in the case of TFA (trifluoroacetate, a negative counterion generally used in cationic peptide synthesis) containing peptides, the use of Raman scattering seems more convenient compared to IR absorption. In fact, TFA anions barely contribute to the amide I region of Raman spectra, rendering less difficult the secondary structural assignments of peptides.[14]

II. Materials and Methods

Three cationic peptides with a generic sequence defined as (KL)$_n$K were synthesized at the Institut Pasteur (Paris) following a solid-phase Fmoc procedure as previously described in detail.[14] They correspond to the values of $n = 1$ (a 3-mer, KLK), $n = 4$ (a 9-mer, KLKLKLKLK), and $n = 7$ (a 15-mer, KLKLKLK-LKLKLKLK). All peptides contain TFA anions. CD and Raman spectra were recorded on purified lyophilized samples dissolved in phosphate buffer containing 10 mM of K^+ and Na^+ cations (pH or pD 6.8). Solutions in D_2O (>99.8% purity, Euriso-Top CEA, France) were prepared under a dry air atmosphere.

CD and Raman setups were described extensively in our recent papers.[1,11,14] Samples used for recording Raman spectra were placed in a quartz suprasil microcell of 35 μL inner volume and excited with the 488 nm line of an Ar^+ laser. Stokes Raman spectra were analyzed at room temperature in the 1750−650 cm^{-1} region (20 min of accumulation, spectral resolution 1 cm^{-1}). To obtain a suitable signal/noise ratio, Raman spectra were recorded at high peptide concentration (ca. 5 mM) whereas CD signals could be measured in the 100 μM to 5 mM range, enabling us to verify an eventual relationship between a peptide concentration and its secondary structure. CD spectra were recorded in a suprasil quartz cell (0.01 or 1 mm path lengths) in the 190−280 nm region. Each spectrum corresponds to an average of five scans with a speed of 100 nm/min (5 min of accumulation). Normalized ellipticity is expressed in deg cm^2 dmol^{-1}.[1]

For the 3-mer and 9-mer, the solubility in aqueous solution was enough to record optical spectra at high concentration (ca. 5 mM), whereas in the case of the 15-mer, a *foamy* solution containing bubbles was obtained at high peptide concentrations. Nevertheless, we observed a gradual disappearing of bubbles a few hours after sample preparation, enabling us to record Raman spectra with a reasonable scattering background. It should be noticed that the addition of methanol to the aqueous solution leads to a better solubilization of the 15-mer. However, solution samples used for recording Raman spectra were prepared without using methanol.

CD and Raman spectra of the 15-mer were recorded as a function of temperature to analyze the structural stability and eventual conformational transitions. However, due to the technical difficulties, the analysis of CD spectra as a function of

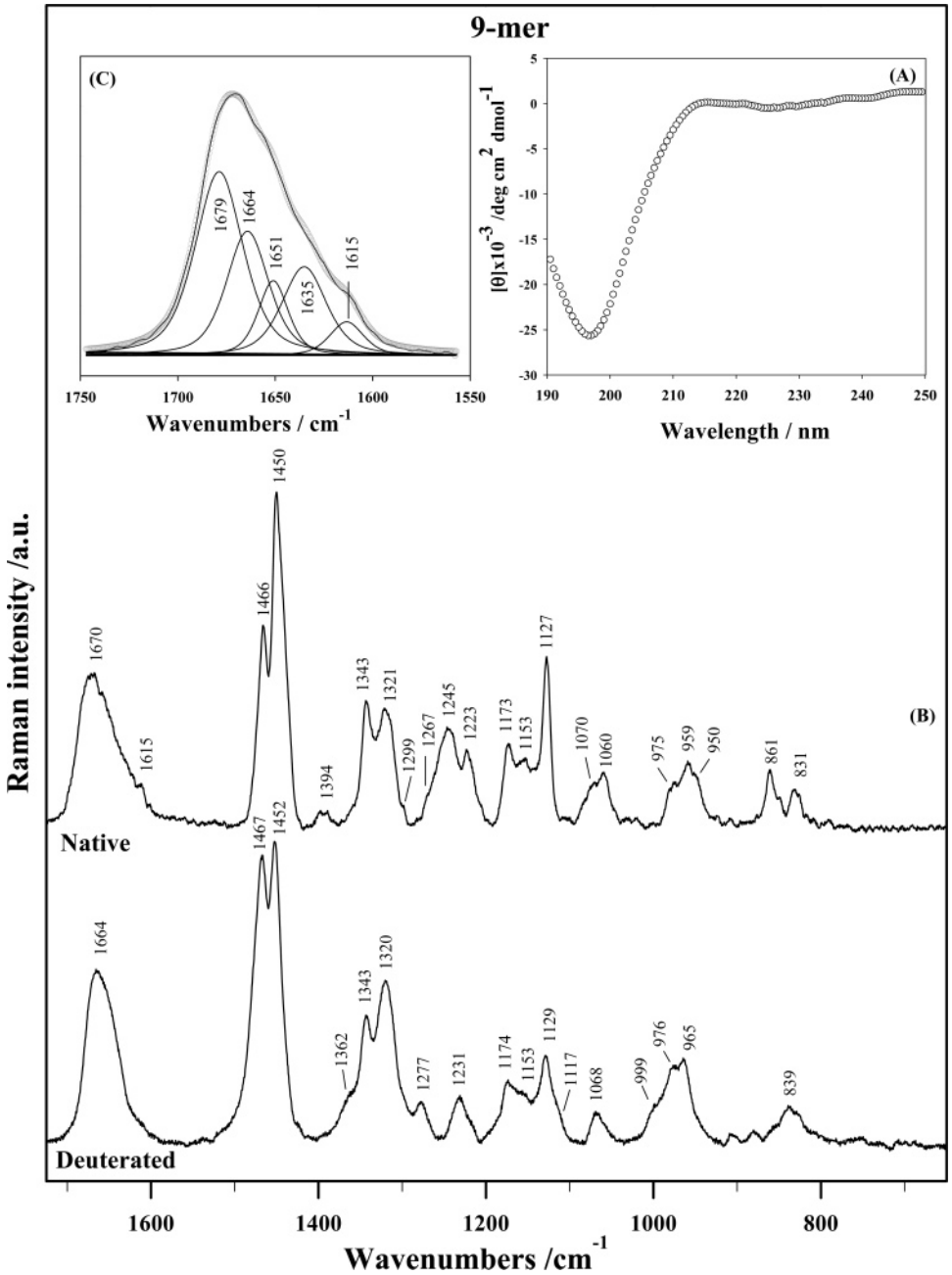

Figure 2. Room-temperature CD and Raman spectra of the 9-mer KLKLKLKLK (5 mM) recorded in phosphate buffer (neutral pH). (A) CD spectrum, (B) comparison between the Raman spectra obtained from native (top) and labile hydrogen deuterated (bottom) species, and (C) Raman band decomposition in the amide I region (native species).

temperature was performed only at 100 μM. Thus, the effect of concentration on the secondary structure could be studied only at room temperature. Curve fitting of the amide I profile in the 1700−1600 cm^{-1} range of Raman spectra was performed by using mixed Gaussian + Lorentzian functions (Lorentzian contribution ≥50%). Initial guesses for their maximum wavenumbers were based on the second derivative analysis in the amide I region. Postprocessing (subtraction of buffer and TFA contributions, baseline correction, and smoothing) was made by GRAMS/32 software (Galactic Industries). Figures are drawn using SIGMAPLOT (Systat Software Inc., Point Richmond, CA) package.

III. Results and Discussion

The CD spectrum of the 3-mer (not shown) is consistent with a disordered chain in aqueous solution.[15,16] Raman spectrum of this peptide (Figure 1) also contains evidence confirming the existence of random chains, especially by the presence of two intense bands at 1684 cm^{-1} (amide I region) and 1254 cm^{-1} (amide III region).[17−19]

Although the CD spectrum of the 9-mer gives a signal traditionally assigned to a disordered chain (intense negative peak at 198 nm, Figure 2A), the amide I region of its Raman spectrum (Figure 2B) shows an intense band at 1670 cm^{-1}. We notice the 14 cm^{-1} downshift of the amide I Raman band of the 9-mer compared to that observed in the 3-mer (1684 cm^{-1}, Figure 1). To obtain further information on the structural evolution of the 9-mer in aqueous solution, we present in Figure 2C the amide I band decomposition of the 9-mer, revealing components assignable to β-type structures, with however a minor component arising from helical conformers (Table 1). Accordingly, the amide III region of the Raman spectrum

TABLE 1: Band Decomposition in the Amide I Region of the Raman Spectra for the Largest Peptides Analyzed in This Work[a]

peptides	apparent position	decomposition	area	BWHH	secondary structure
	1670	1679	50	28	β-turn, random
		1664	21	22	β-strand
KLKLKLKLK		1651	8	16	helix
		1635	16	25	β-sheet
	1615	1615	5	25	
KLKLKLKLKLKLKLK	1669	1669	100	13	β-strand

[a] All band positions are in cm^{-1}. BWHH: bandwidth at half-height (cm^{-1}) of the components. Area of each component is expressed in % (total area of the decomposed region 100%).

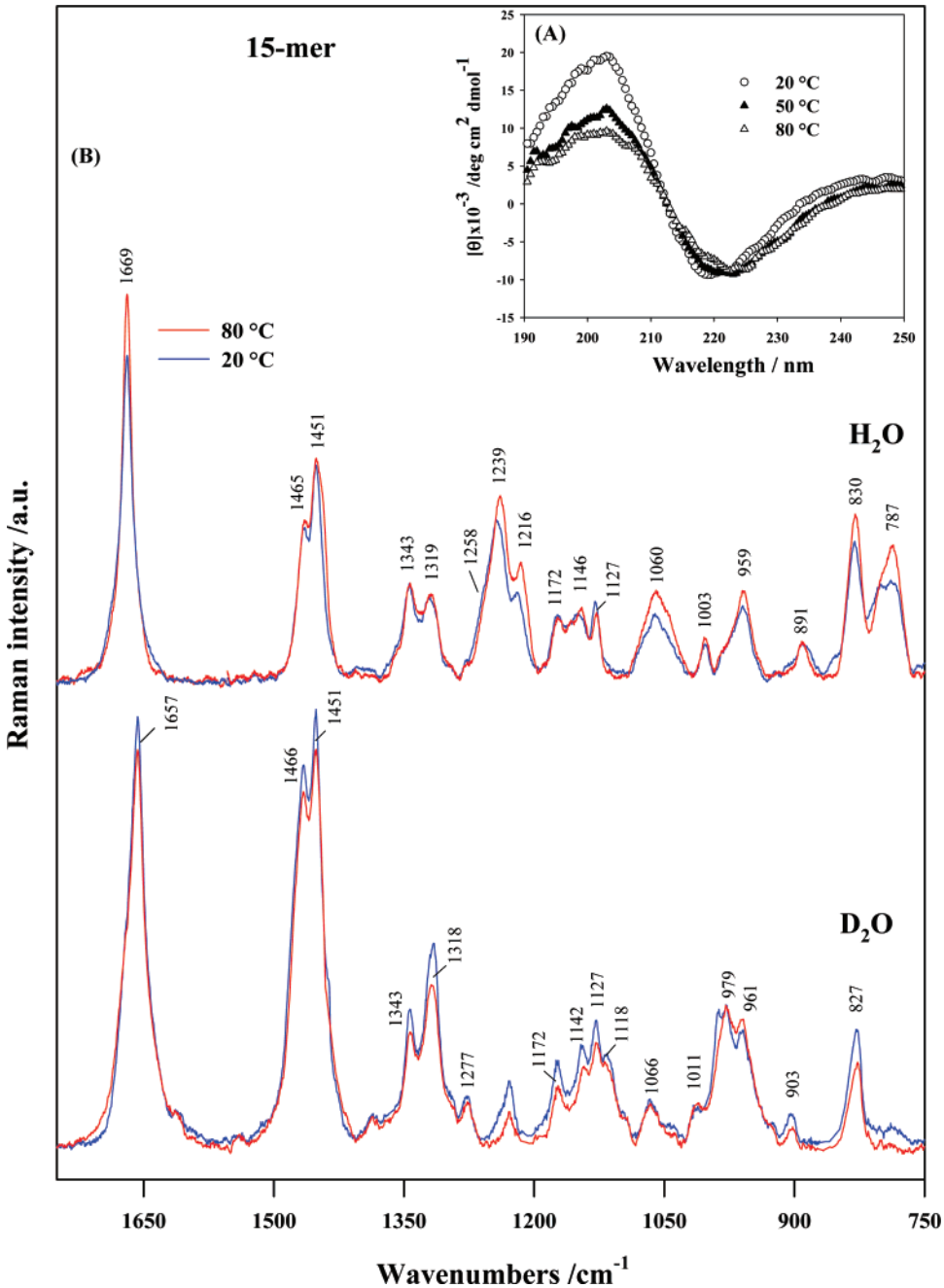

Figure 3. CD and Raman spectra of the 15-mer KLKLKLKLKKLKLK recorded in phosphate buffer. (A) CD spectra as a function of temperature. Due to the technical difficulties, only the variation of CD spectra at 100 μM are presented. Note that CD spectra recorded at room temperature for ultimate concentrations (100 μM and 5 mM) are superposable. (B) Comparison between the Raman spectra (5 mM) obtained from native (top) and labile hydrogen deuterated (bottom) species, at 20 °C (blue trace) and 80 °C (red trace).

(Figure 2B) becomes more structured (compared to that of the 3-mer, Figure 1) with a pronounced peak at 1245 cm^{-1} (β-type conformers), and two shoulders at 1267 cm^{-1} (random chains), and at 1299 cm^{-1} (helical conformers).[17,19,20] Our observations by optical techniques concerning the 9-mer give further evidence on possible misinterpretation of β-family secondary structures

TABLE 2: Peak Position of a Leucine Residue Raman Marker Observed in H_2O and D_2O Buffer of Leucine and Minimalist LK Peptides[a]

molecule	H_2O buffer	D_2O buffer	major conformers[b]	details
L (amino acid)	1134	1129		refs 24 and 25
KLK (3-mer)	1129	1132	R	this report
KLLLK (5-mer)	1127	1132	β, h, R	ref 1
KLKLKLKLK (9-mer)	1127	1129	β, R	this report
KLLKLLLKLLK (11-mer)	1127	1131	β, R, h	ref 1
KLKLKLKLKLKLKLK (15-mer)	1127	1127	β	this report
KLLKLLLKLLLKLLK (15-mer)	1127	1107	h	ref 1
KLLKLLLKLLLKLLLKLLK (19-mer)	1127	1107	h	ref 1

[a] Peak positions are in cm^{-1}. [b] They are mentioned in the decreasing order of their respective populations as determined by the amide I characteristic Raman band. Only those conformers corresponding to a population equal to or greater than 10% (of the total population) are reported. R, h, and β refer to random, helical, and β-type chains, respectively.

TABLE 3: Peak Positions and Tentative Assignments of the Raman Bands Recorded at Room Temperature in Phosphate Buffer from the Three Peptides Studied in This Work[a]

3-mer		9-mer		15-mer		tentative assignments
1684 (s)	1670 (s)					
1660 (sh)		1670 (s)	*1664 (s)*	1669 (s)	*1657 (s)*	amide I
		1615 (sh)				
1467 (s)	*1467 (s)*	1466 (s)	*1467 (s)*	1465 (s)	*1466 (s)*	side chain, CH_3 and CH_2 bend
1451 (s)	*1453 (s)*	1450 (s)	*1452 (s)*	1451 (s)	*1451 (s)*	
1388 (w)	*1394 (w)*	1394 (w)				
	1363 (m)		*1362 (sh)*		*1362 (w)*	
1343 (s)	*1344 (s)*	1343 (s)	*1343 (s)*	1343 (s)	*1343 (s)*	side chain, CCH bend, C_α-bend
1321 (s)	*1321 (s)*	1321 (s)	*1320 (s)*	1319 (s)	*1318 (s)*	
1281 (w)		1299 (sh)				
	1274 (w)		*1277 (m)*		*1277 (w)*	amide III
1254 (m)		1267 (sh)		1258 (sh)		
		1245 (s)		1239 (s)		
			1231 (m)			
1224 (m)	*1225 (m)*	1223 (m)		1216 (s)		backbone
1204 (w)	*1200 (w)*					
1174 (m)	*1173 (m)*	1173 (m)	*1174 (m)*	1172 (m)	*1172 (m)*	
1143 (m)	*1155 (w)*	1153 (m)	*1153 (m)*	1146 (m)	*1142 (m)*	side chain, CH_2 twist, C_α-bend
1129 (s)	*1132 (m)*	1127 (s)	*1129 (m)*	1127 (m)	*1127 (m)*	
	1109 (sh)		*1117 (sh)*		*1118 (sh)*	
1074 (m)	*1070 (m)*	1070 (sh)	*1068 (m)*			side chain, CC str.
1061 (m)		1060 (m)	*1067 (w)*	1060 (m)	*1066 (w)*	
1020 (w)	*1019 (sh)*				1011 (w)	
	1003 (m)		*999 (sh)*	1003 (w)		
980 (sh)		975 (sh)	*976 (m)*		*979 (s)*	
963 (m)	*970 (s)*	959 (m)	*965 (m)*	959 (m)	*961 (s)*	side chain, CH_3 rock
945 (sh)	*949 (sh)*	950 (sh)				
903 (w)				891 (w)	*903 (w)*	
	883 (w)					
862 (m)		861 (m)				side chain, CH_2 wag, CC str
	844 (w)		*839 (m)*			
		831 (m)		830 (s)	*827 (m)*	
831 (s)						
	811 (w)					
784 (m)	*783 (w)*			787 (s)		backbone, N−C−C bend
732 (w)	*732 (w)*					

[a] 3-mer: KLK. 9-mer: KLKLKLKLK. 15-mer: KLKLKLKLKLKLKLK. s: intense. m: middle. w: weak. sh: shoulder. In italics are reported the peak positions in D_2O buffer.

by CD measurements alone. In fact, extended loops and strands may be assigned to unordered elements.[16,21−23]

On going from the 9-mer to the 15-mer, the CD spectrum takes a shape which can undoubtedly be assigned to β-type conformers (strong negative peak at ca. 220 nm, Figure 3A).[14−16,21] The Raman spectrum of this peptide shows a strong amide I band at 1669 cm^{-1}. The symmetrical shape of this band allows us to cover the quasi whole of its area by a single and narrow band at the same wavenumber (Table 1). It should be emphasized that a Raman band observed around 1665 cm^{-1} is generally assigned to nonassociated (by means of H-bonds) β-strands.[17,20] The amide III region contains a pronounced peak at 1239 cm^{-1}, also consistent with a major population of β-type conformers in solution.[19] However, a shoulder at 1257 cm^{-1} allows us to presume a small proportion of random conformers, despite the absence of any observable random marker counterpart in the amide I region.

Labile hydrogen deuteration reveals a general downshift (about 10 cm^{-1} in average) of the apparent peak observed in the amide I region (1700−1600 cm^{-1}) accompanied by the

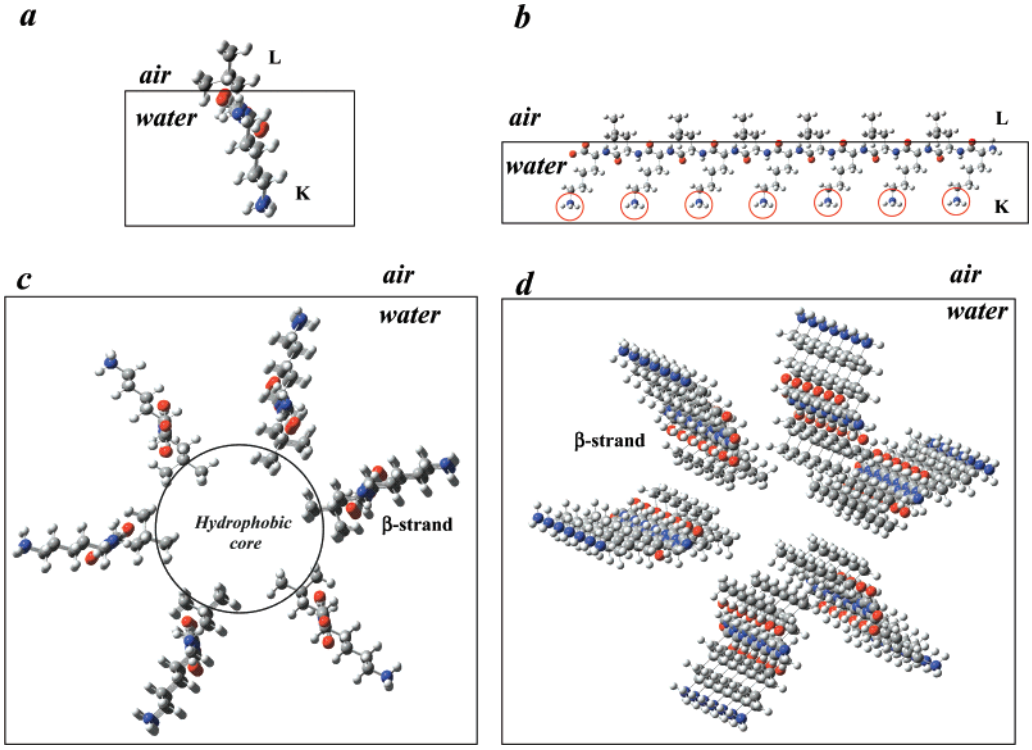

Figure 4. Graphic presentation of the 15-mer KLKLKLKLKLKLKKK and its probable aggregates. (Left) The 15-mer adopting an ideal β-strand conformation viewed parallel (a) and (b) perpendicular to the backbone axis direction. Charged heads (NH_3^+) of lysines are surrounded by red circles (b). An ideal symmetrical immiscible aggregate formed by six β-strands, seen parallel to (c), or with an angle with respect to (d), the aggregate axis. Hydrophobic core of the aggregate is surrounded by a black circle (c). Nitrogen in blue, oxygen in red, carbon in gray, and hydrogen in white.

vanishing of the amide III markers observed in the 1300−1230 cm^{-1} region (Figures 1, 2B, and 3B). These effects are currently observed in peptides upon N−H deuteration. Other substantial changes observed in the region below 1200 cm^{-1} also lead us to conclude that a complete deuteration on labile hydrogens was achieved in D_2O buffer. Consequently, no intra- or intermolecular H-bonding could avoid or retard H−D substitutions on labile hydrogens. It should also be noted that, as expected, apart from some changes in relative intensities of Raman bands, a much less pronounced deuteration effect is observed on the modes originating from the CH_3 and CH_2 groups of leucine and lysine side chains (strong bands located in the 1470−1450 and 1350−1315 cm^{-1} spectral regions). In the second manuscript of this series,[1] we could emphasize the special behavior of a characteristic leucine residue vibrational mode upon deuteration, through the examination of the 1134−1127 cm^{-1} region of the Raman spectra observed in aqueous samples of leucine[24,25] and LK peptides with KLL(KLLL)$_n$KLLK primary sequences[1] (see Table 2 for a review). The analysis of the eight examples reported previously[1,24] and in this report (Table 2) allows us to emphasize the following: (i) the mode observed in the leucine spectrum at 1134 cm^{-1} is downshifted to ca. 1127 cm^{-1} when leucine residue is inserted in a peptide chain; (ii) the isotopic shift of the ∼1127 cm^{-1} mode is conformational-dependent; i.e., in the short peptide chains (from 3-mer to 11-mer) where a mixture of several conformers is present in solution, this mode gives rise to a slight upshift varying from 2 to 5 cm^{-1}, in perfectly helical chains it gives rise to a considerable downshift to 1107 cm^{-1}, and finally in a β-type chain (such as those corresponding to the 9-mer and 15-mer) the isotopic downshift decreases upon increasing chain length (2 cm^{-1} in the 9-mer, nonobservable in the 15-mer, Table 2). Consequently, upon isotopic shift observations mentioned above (Table 2), we can assume that the coupling of the above-mentioned leucine mode with the backbone vibrational motions increase in the following order as a function of peptide secondary structure: helical chain > disordered chain > β-strand (Table 2).

All observed Raman peaks of the peptides studied in this work and their tentative assignments are reported in Table 3.

The analysis of CD and Raman spectra of the 15-mer as a function of temperature are also displayed in Figure 3. CD spectra recorded in the 20−80 °C temperature range (Figure 3A) show a slight decrease of the positive peak at ca. 200 nm, without an observable change in the negative peak at 220 nm (β-type CD marker). We interpret this shape change by an increase of random chain population with temperature. In fact, the decrease of the signal around 200 nm should be the result of compensation between the negative random chain signal (at 198 nm) and the positive low-wavelength tail of the β-type signal (at 200 nm). In Figure 3B we also show the superposition of the Raman spectra of the 15-mer obtained at the two ultimate temperatures (20 and 80 °C). Apart from some little changes in the intensity of Raman bands, no characteristic wavenumber change could be measured upon such an important temperature variation (Δt = 60 °C), especially in the amide I and amide III regions (both regions are sensitive to peptide conformation, as well as to intra- and interchain H-bonding). Therefore, we conclude that the 15-mer is present in solution as highly stable β-strands with possible aggregation but surely not stabilized by means of interstrand H-bonds.

IV. Concluding Remarks

In this report and in an accompanying one,[1] we have shown the advantage of the joint use of CD and Raman structural markers for a better understanding of structural behavior minimalist cationic LK peptides in aqueous solution. Two series of peptides have been studied, those with KLLL repeat, precisely

with KLL(KLLL)$_n$KLLK primary sequence,[1] and the others with KL repeat (this work), that show a natural tendency to adopt ordered unique structures upon increasing chain length, i.e., α-helical and β-type conformers in the first and second subfamilies of LK peptides, respectively).

An overview of all the results reported in the present work to emphasize the main remarks follows:

(a) For a sufficient length, i.e., 15 residues ($n = 7$), a peptide with KL repeat adopts non-H-bonded β-strands in phosphate buffer. This conclusion could be derived on the basis of optical spectra as a function of temperature (vide supra). The environment dependence of the conformational equilibrium of these peptides was reported previously.[14] Particularly, the following has been emphasized: (i) the capability of the 9-mer ($n = 4$) and the 15-mer ($n = 7$) to adopt non-native helical secondary structures in methanol and in methanol/tris mixture, (ii) a helical to β-type transition appearing in solution with a time delay depending on the peptide concentration, (iii) the stabilization of helical conformers in a methanol/tris mixture at low concentrations (<100 μM), and (iv) the formation of β-type conformers in PBS and in a methanol/PBS mixture without any measurable interconversion toward helical ones. Consequently, we can postulate that phosphate anions (present both in phosphate buffer and in PBS) have a considerable effect on the stabilization of β-strands, presumably through a possible screening of positively charged lysine side chains, thus decreasing their electrostatic repulsive interactions.

(b) We now have sufficient data to reconsider the assumptions made previously on the secondary structure of the peptides with KL repeat. Especially, it is difficult to accept that the 15-mer (KL)$_7$K adopts, as postulated before,[8] an antiparallel β-sheet structure independently from environment and concentration.

In fact, β-strands formed by the 15-mer are *amphipathic* chains with leucine side chains (hydrophobic) located on one side and the lysine side chains (hydrophilic) on the other side (Figures 4a and 4b). This model is perfectly in agreement with the assumptions made previously on the flat orientation of the peptide chains at the air/water interface[8] because they were collected at low peptide concentrations (sub-micromolar). When the number of peptide molecules increases (high peptide concentrations), the problem of low solubility of β-strands may consequently appear. We have mentioned (in the Materials and Methods section) that the 15-mer gives rise to *foamy solutions*, especially at high peptide concentrations (5 mM, necessary for recording Raman spectra), with however a gradual evolution toward a transparent solution with time. This effect cannot be described by the formation of β-sheet structures (H-bonded β-strands) at the air/water interface (see above our conclusion from the Raman spectra as a function of temperature). Another model of aggregation based on the interaction of peptide strands through hydrophobic interaction seems to be more adequate for explaining the nonsolubility of the 15-mer at high concentrations. A hypothetic model with six interacting β-strands is displayed in Figures 4c and 4d. Hydrophobic interactions via leucine side chains, as well as hydrophilic interactions through the positively charged lysine side chains (oriented toward water molecules), can lead to the gradual solubilization of such a supermolecular structure. However, some further investigations by means of fluorescence spectroscopy,[26] atomic force microscopy, and molecular dynamics simulations are necessary to validate such a hypothetical aggregate model (Figure 4). In some LK peptides with antimicrobial effect, it has been shown that the aggregation leads to the inactivation of peptides in solution (see ref 27 for a review). L/D enantiomeric replacement in some residues along the chain has shown to avoid aggregation and enhance the antimicrobial effects of LK peptides.[26]

(c) Another interesting point that could be elucidated in this work is the difficulty encountered again in assigning the secondary structure of the peptides on the basis of CD spectra alone.[16,21,22,28,29] For instance, the 9-mer, which gives rise to a disordered CD signal, is shown to adopt several types of secondary structures in solution, predominantly corresponding to β-like conformers (Raman data). In fact, the enveloping (average) CD signal arising from several secondary conformers may resemble in many cases that traditionally assigned to random chains in solution. Theoretical attempts to calculate the CD signals from molecular dynamics trajectories have revealed that several conformers obtained during a long period of simulations are necessary to reproduce satisfactorily the observed data in short peptides.[30]

(d) We can recall here the results reported previously[31] from some (LK)$_n$ and (LKKL)$_n$ peptides as a function of ionic strength and molecular concentration, which show their tendency to adopt β-type and helical conformations, respectively. This allows us to conclude that the replacement of L by K (and inversely) in both types of peptides, i.e., with KL and KLLL repeats, has presumably a secondary effect on their conformations appearing in aqueous solution.

References and Notes

(1) Guiffo-Soh, G.; Hernandez, B.; Coïc, Y. M.; Boukhalfa-Heniche, F. Z.; Ghomi M. *J. Phys. Chem. B* **2007**, 111, 12563−12572.
(2) Blondelle, S.; Houghten, R. A. *Biochemistry* **1992**, *31*, 12688−12694.
(3) Cornut, I.; Buttner, K.; Dasseux, J. L.; Dufourcq, J. *FEBS Lett.***1994**, *349*, 29−33.
(4) Dufourcq, J.; Neri, W.; Henry-Toulmé, N. *FEBS Lett.* **1998**, *421*, 7−11.
(5) Niidome, T.; Takaji, K.; Urakawa, M.; Ohmori, N.; Wada, A.; Hirayama, T.; Aoyagi, H. *Bioconjugate Chem.* **1999**, *10*, 773−780.
(6) Castano, S.; Cornut, I.; Buttner, K.; Dasseux, J. L.; Dufourcq, J. *Biochim. Biophys. Acta* **1999**, *1416*, 161−175.
(7) Castano, S.; Desbat, B.; Laguerre, M.; Dufourcq, J. *Biochim. Biophys. Acta* **1999**, *1416*, 176−194.
(8) Castano, S.; Desbat, B.; Dufourcq, J. *Biochim. Biophys. Acta* **2000**, *1463*, 65−80.
(9) Maget-Dana, R.; Lelievre, D. *Biopolymers* **2001**, *59*, 1−10.
(10) Béven, L.; Castano, S.; Dufourcq, J.; Wieslander, A.; Wroblewski, H. *Eur. J. Biochem.* **2003**, *270*, 2207−2217.
(11) Boukhalfa-Heniche, F. Z.; Hernandez, B.; Gaillard, S.; Coïc, Y. M.; Huynh-Dinh, T.; Lecouvey, M.; Seksek, O.; Ghomi, M. *Biopolymers* **2004**, *73*, 727−734.
(12) Blondelle, S. E.; Lohner K.; Aguilar, M. I. *Biochim. Biophys. Acta* **1999**, *1462*, 89−108.
(13) Escrive, C.; Laguerre, M. *Biochim. Biophys. Acta* **2001**, *1513*, 63−74.
(14) Hernandez, B.; Boukhalfa-Heniche, F. Z.; Seksek, O.; Coïc, Y. M.; Ghomi, M. *Biopolymers* **2006**, *81*, 8−19.
(15) Chou, P. Y.; Fasman, G. D. *Biochemistry* **1974**, *13*, 211−222.
(16) Brahms, S.; Brahms, J. *J. Mol. Biol.* **1980**, *138*, 149−178.
(17) Krimm, S.; Bandekar, *J. Adv. Protein Chem.* **1986**, *38*, 181−164.
(18) Le Bihan, T.; Blochet, J. E.; Desormeaux, A.; Marion, D.; Pezolet, M. *Biochemistry* **1996**, *35*, 12712−12722.
(19) Carey, P. R. *Biochemical Application of Raman and Resonance Raman Spectroscopies*; Academic Press: New York, 1982.
(20) Maiti, N. C.; Apetri, M. M.; Zagorski, M. G.; Carey, P. R.; Anderson, V. E. *J. Am. Chem. Soc.* **2004**, *126*, 2399−2408.
(21) Surewicz, W. K.; Mantsch, H. H.; Chapman, D. *Biochemistry* **1993**, *32*, 389−394.
(22) Dong, A.; Kendrick, B.; Kreilgard, L.; Matsuura, J.; Manning, M. C.; Carpenter, J. F. *Arch. Biochem. Biophys.* **1997**, *347*, 213−220.
(23) Altman, M.; Lee, P.; Rich, A.; Zhang, S. *Protein Sci.* **2000**, *9*, 1095−1105.
(24) Overman, S. A.; Thomas, G. J., Jr. *Biochemistry* **1998**, *37*, 5654−5665.

(25) Derbel, N.; Hernandez, B.; Pflüger, F.; Liquier, J.; Geinguenaud, F.; Jaidane, N.; Lakhdar, Z. B.; Ghomi, M. *J. Phys. Chem. B* **2007**, *111*, 1470−7.

(26) Avrahami, D.; Oren Z.; Shai, Y. *Biochemistry* **2001**, *40*, 12591−12603.

(27) Shai, Y. *Curr. Pharm. Des.* **2002**, *8*, 715−725.

(28) Pelton, J. T.; McLean, L. R. *Anal. Biochem.* **2000**, *277*, 167−176.

(29) Yada, R. Y.; Jackman, R. L.; Nakai, S. *Int. J. Peptide Protein Res.* **1988**, *31*, 98−108.

(30) Glattli, A.; Daura, X.; Seebach, D.; van Gunsteren, W. F. *J. Am. Chem. Soc.* **2002**, *124*, 12972−12978.

(31) Baumruk, V.; Huo, D.; Dukor, R. K.; Keiderling, T. A.; Lelievre, D.; Brack, A. *Biopolymers* **1994**, *34*, 1115−1121.